

# Selfconsistent approximations, symmetries and choice of representation

Stefan Leupold

*Institut für Theoretische Physik, Universität Giessen, Germany*

In thermal field theory selfconsistent ( $\Phi$ -derivable) approximations are used to improve (resum) propagators at the level of two-particle irreducible diagrams. At the same time vertices are treated at the bare level. Therefore such approximations typically violate the Ward identities connected to internal symmetries. Examples are presented how such violations can be tamed by a proper choice of representation for the fields which describe the system under consideration. These examples cover the issue of massless Goldstone bosons in the linear sigma model and the Nambu–Jona-Lasinio model and the problem of current conservation in theories with massive vector mesons.

PACS numbers: 11.10.Wx,11.30.-j,11.30.Rd

Keywords: Selfconsistent approximations, symmetries, thermal field theory

## I. INTRODUCTION AND SUMMARY

For the description of quantum field theories in and also out of thermal equilibrium  $\Phi$ -derivable approximations [1, 2, 3] have gained a lot of attention in the last years [4, 5, 6, 7, 8, 9, 10, 11, 12, 13, 14, 15, 16, 17, 18, 19, 20, 21, 22, 23, 24, 25, 26, 27]. Such an approach provides a tool to go beyond purely perturbative calculations by resumming whole classes of diagrams. At the same time the approximation scheme is thermodynamically consistent [1, 5]. Typically the generating functional which defines the approach is introduced as a functional of one- and two-point functions (classical fields and propagators). Consequently, the key quantity  $\Phi$  is calculated from two-particle irreducible (2PI) diagrams (see e.g. [20] for a generalization to  $n$ -PI diagrams). In this way, one deals with full propagators, while vertices are treated at a perturbative level. If the system under consideration contains internal symmetries, such an approach can violate the Ward identities connected to these symmetries [9]. The reason is that Ward identities typically connect propagators and vertices. Therefore, problems can occur in a scheme in which propagators are determined by involving diagrams of arbitrary loop order, while vertices are calculated only up to a given loop order.

The purpose of the present work is to show some examples where such problems appear and to point out how these problems can be avoided by a proper redefinition of fields. The present work does *not* aim at a full formal solution of arbitrary problems connected to resummations in the presence of internal symmetries. Rather for some examples of practical relevance (Goldstone modes, current conservation in theories with massive vector mesons), it is shown how the problems can be tamed. Also the discussion of renormalization issues (cf. e.g. [7, 8, 9]) is beyond the scope of the present work.

In principle, physical quantities (e.g.  $S$ -matrix elements) do not depend on the choice of representation [28, 29]. Thus, it is important to understand why a redefinition of fields, i.e. a clever choice of representation can help at all: The point is that typically one cannot calculate a physical quantity exactly, i.e. one does not have a full solution to the quantum field theoretical problem, but only an approximation. E.g. in a perturbation theory differences originating from different choices of representation are of higher order in the expansion parameter than the order studied (see e.g. [30] and references therein). In resummation schemes one typically involves classes of processes/diagrams up to infinite order in the expansion parameter (e.g. two-particle reducible diagrams) while other classes are treated perturbatively. In such a scheme the only thing one can say about the (in-)dependence on the choice of representation is that the results should become less dependent on the representation, if one includes more and more processes/diagrams (in a systematic way). Therefore, in practice where one cannot solve the full quantum field theoretical problem, the choice of representation might matter. As will be outlined in the present work it can indeed be used as a tool to improve the symmetry properties of a resummation scheme.

The rest of the present work is structured as follows: In the next section we discuss the linear sigma model and in section III the Nambu–Jona-Lasinio model. In both sections we focus on the problem that the propagator of the (supposed-to-be) Goldstone bosons might not propagate massless modes, if it is calculated within a  $\Phi$ -derivable approximation with resummed propagators but bare vertices. We will show that such a problem appears, if a linear representation for the Goldstone boson fields is used, whereas Goldstone modes remain massless for a non-linear representation. Note that a similar line of reasoning is also presented in [31], however not in the context of  $\Phi$ -derivable schemes. For the Nambu–Jona-Lasinio model also a redefinition of the quark fields will be important on top of the change of representation for the Goldstone boson fields. In section IV we turn to a different problem, namely the current (non-)conservation in theories with massive vector mesons. Here it will turn out that the use of a tensor representation for the vector mesons is superior to the frequently used vector representation. We will also present a projector formalism which deals with the technical aspects of the tensor representation. As a side remark on the

treatment of tadpoles in  $\Phi$ -derivable schemes we have added an appendix.

## II. LINEAR SIGMA MODEL

As a first example we take the  $O(N + 1)$  linear sigma model [32]

$$\mathcal{L} = \frac{1}{2} \partial_\mu \vec{\phi} \partial^\mu \vec{\phi} + \frac{1}{2} m^2 \vec{\phi}^2 - \frac{\lambda}{4} (\vec{\phi}^2)^2. \quad (1)$$

Here  $\vec{\phi}$  is a  $N + 1$  component vector (linear representation)

$$\vec{\phi} = \begin{pmatrix} \phi_0 \\ \vdots \\ \phi_N \end{pmatrix}. \quad (2)$$

The Lagrangian (1) is invariant with respect to the global transformations

$$\vec{\phi} \rightarrow S \vec{\phi} \quad (3)$$

with an arbitrary matrix  $S \in O(N + 1)$ .

For  $m^2 > 0$  (and low enough temperatures) the system described by (1) has a non-trivial ground state which spontaneously breaks the symmetry (3). We choose the (positive)  $\phi_0$  direction and find:

$$\phi_0^{\text{vac}} = \sqrt{\frac{m^2}{\lambda}} =: v. \quad (4)$$

To study the (quantum and thermal) fluctuations around this ground state we perform a shift in (1)

$$\phi_0 \rightarrow v + \phi_0 \quad (5)$$

which yields the Lagrangian

$$\mathcal{L}_{\text{lin. repr.}} = \frac{1}{2} \partial_\mu \vec{\phi} \partial^\mu \vec{\phi} - \frac{\lambda}{4} (\vec{\phi}^2)^2 - \frac{1}{2} m_0^2 \phi_0^2 - \lambda v \phi_0 \vec{\phi}^2 \quad (6)$$

with the mass for the  $\phi_0$  mode

$$m_0^2 := 2\lambda v^2 = 2m^2. \quad (7)$$

Note that the spontaneous symmetry breaking induces a new three-point interaction term, the last term on the right hand side of (6).

Spontaneously broken global symmetries cause the appearance of massless Goldstone modes [32, 33]. For the studied system these are the  $\phi_i$  ( $i \neq 0$ ) modes. Indeed, on the tree level there are no mass terms for the  $\phi_i$  modes. Single loop diagrams induce mass terms. In a perturbative expansion, however, such mass terms cancel in the sum of all contributing loop diagrams. An example of such a cancellation is depicted in figure 1. There, all one-loop self

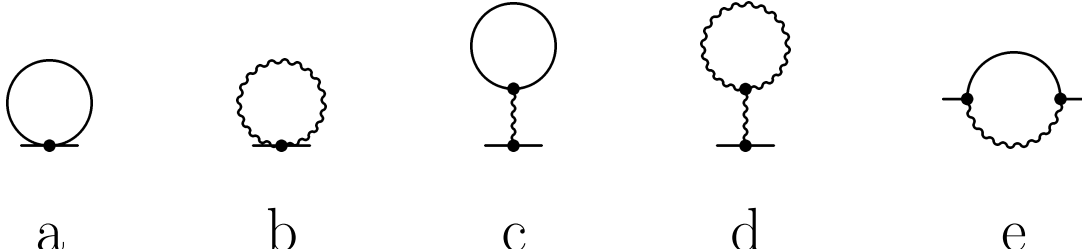


FIG. 1: Self energy contributions which — in a perturbative treatment — conspire such that no mass terms are induced. Solid lines denote  $\phi_i$  modes ( $i \neq 0$ ), wiggly lines  $\phi_0$  modes. See main text for details.

energy diagrams for the  $\phi_i$  modes are shown. The sum of these contributions is proportional to  $I_a + I_b + I_c + I_d + I_e$  with the  $\phi_i$  snail diagram

$$I_a = \lambda (N+2) \oint \frac{d^4 p}{(2\pi)^4} \frac{1}{p^2}, \quad (8)$$

the  $\phi_0$  snail diagram

$$I_b = \lambda \oint \frac{d^4 p}{(2\pi)^4} \frac{1}{p^2 - m_0^2}, \quad (9)$$

the  $\phi_i$  tadpole

$$I_c = (\lambda v)^2 2N \frac{1}{-m_0^2} \oint \frac{d^4 p}{(2\pi)^4} \frac{1}{p^2} = -\lambda N \oint \frac{d^4 p}{(2\pi)^4} \frac{1}{p^2}, \quad (10)$$

the  $\phi_0$  tadpole

$$I_d = 6 (\lambda v)^2 \frac{1}{-m_0^2} \oint \frac{d^4 p}{(2\pi)^4} \frac{1}{p^2 - m_0^2} = -3\lambda \oint \frac{d^4 p}{(2\pi)^4} \frac{1}{p^2 - m_0^2} \quad (11)$$

and the  $\phi_i$ - $\phi_0$  loop

$$I_e(k) = 4 (\lambda v)^2 \oint \frac{d^4 p}{(2\pi)^4} \frac{1}{(p^2 - m_0^2)(p - k)^2} = 2\lambda m_0^2 \oint \frac{d^4 p}{(2\pi)^4} \frac{1}{(p^2 - m_0^2)(p - k)^2}. \quad (12)$$

We have introduced the Matsubara formalism [34] to calculate the diagrams at finite temperature. In the following, our considerations will be at a purely formal level. Therefore we are not concerned with the renormalization of the expressions in (8)-(12).

A mode remains massless, if the corresponding self energy  $\Pi$  satisfies

$$\lim_{k \rightarrow 0} \Pi(k) = 0. \quad (13)$$

The following decomposition for diagram (e) ensures that the  $\phi_i$  modes remain massless:

$$\frac{m_0^2}{(p^2 - m_0^2)(p - k)^2} = \frac{1}{p^2 - m_0^2} - \frac{1}{(p - k)^2} - \frac{-2kp + k^2}{(p^2 - m_0^2)(p - k)^2} \quad (14)$$

i.e. the first two terms on the right hand side of (14) cancel the result of the sum of  $I_a + I_b + I_c + I_d$  whereas the last term vanishes with the external momentum  $k$ .

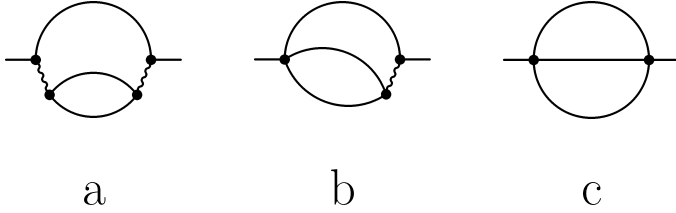


FIG. 2: Some two-loop self energy contributions for the linear sigma model. Solid lines denote  $\phi_i$  modes ( $i \neq 0$ ), wiggly lines  $\phi_0$  modes.

With the decomposition (14) one basically transforms two propagators to one propagator, i.e. one contracts one propagator in diagram 1(e). The remaining piece vanishes with the external momentum, i.e. does not play a role. By the contraction of one propagator diagram 1(e) looks the same as diagram 1(a) or (b), respectively, depending which propagator is contracted. Also at higher loop order corresponding cancellations happen between diagrams which differ from each other by one propagator. As an illustrative example suppose that one wants to consider the two-loop diagram shown in figure 2(a). To ensure that the mode remains massless one needs in addition (besides others) the diagrams depicted in figure 2(b) and (c).

This rather subtle cancellation does not work any longer once the propagators are dressed. In the following, we will demonstrate the problem in two ways. Suppose that we calculate the  $\phi_i$  propagators according to a  $\Phi$ -derivable

approximation using for  $\Phi$  the two-loop diagrams depicted in figure 3.<sup>1</sup> This approach generates all self energies

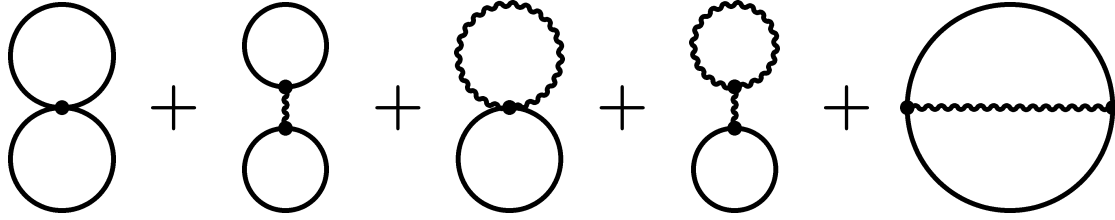


FIG. 3: Contributions to the  $\Phi$ -functional (relevant for the generation of  $\phi_i$  self energies) in two-loop order for the linear sigma model (in linear representation). Solid lines denote  $\phi_i$  modes ( $i \neq 0$ ), wiggly lines  $\phi_0$  modes. See main text for details.

shown in figure 1 with the important difference that now all internal lines should be regarded as full instead of bare propagators.<sup>2</sup> The necessary cancellation between diagram (e) and the sum of the others would still take place, *if* the following difference vanished with the external momentum  $k$  (cf. equation (14)):

$$\Delta := \frac{m_0^2}{[p^2 - m_0^2 - \Pi_0(p)][(p - k)^2 - \Pi_i(p - k)]} - \left( \frac{1}{p^2 - m_0^2 - \Pi_0(p)} - \frac{1}{(p - k)^2 - \Pi_i(p - k)} \right), \quad (15)$$

where we have introduced self energies  $\Pi_0$  and  $\Pi_i$  for the  $\phi_0$  and  $\phi_i$  modes, respectively. Instead of an expression which vanishes with  $k$  we get

$$\Delta = \frac{2kp - k^2 + \Pi_i(p - k) - \Pi_0(p)}{[p^2 - m_0^2 - \Pi_0(p)][(p - k)^2 - \Pi_i(p - k)]} \xrightarrow{k \rightarrow 0} \frac{\Pi_i(p) - \Pi_0(p)}{[p^2 - m_0^2 - \Pi_0(p)][p^2 - \Pi_i(p)]}. \quad (16)$$

In general, the right hand side of (16) does not vanish, since the self energies  $\Pi_0$  and  $\Pi_i$  are not the same. E.g. the self energy for the  $\phi_0$  mode has an imaginary part coming from the decay into two (ideally massless)  $\phi_i$  modes. This decay channel is not present for a  $\phi_i$  mode.

There is a second way to see that the cancellation does not work any more. For that purpose we work out which *perturbative* diagrams are generated from the  $\Phi$  functional of figure 3 and which are not. Obviously, one generates (besides infinitely many other perturbative diagrams) the (perturbative!) two-loop self energy shown in figure 2(a). (Note that the lines in figure 3 denote *full* propagators, whereas the lines in figure 2 denote *bare* propagators.) On the other hand, the diagrams depicted in figure 2(b) and (c) are *not* generated from  $\Phi$  as given in figure 3. Three-loop diagrams for  $\Phi$  would be necessary here. As already pointed out, all diagrams of figure 2 would be needed to ensure that the  $\phi_i$  modes remain massless at the two-loop level.

More generally, the symmetries (which dictate the appearance of Goldstone modes) lead to Ward identities which typically connect propagators and vertices. If one resums propagators to all orders but truncates the vertices, one might get problems, since the necessary cancellation of different diagrams is not ensured any longer. Note that e.g. diagram 2(a) is a propagator correction to diagram 1(e), while diagram 2(b) is a vertex correction. Also note that the inclusion of diagram 2(b) — even with full propagators — would not solve the problem in a 2PI  $\Phi$ -derivable scheme: Using full propagators one would need a *full* vertex and not just bare plus one-loop.

The previous discussion shows that one has to look for a formalism where such cancellations are not needed. To see that this is indeed possible and practically conceivable we turn to the non-linear representation (see e.g. also [31])

$$\vec{\phi} = \sigma \vec{U} \quad (17)$$

with  $\vec{U}^2 = 1$ . Obviously, as a unit vector in  $N + 1$  dimensions,  $\vec{U}$  contains  $N$  degrees of freedom which we will call “ $\pi$  modes” in the following. In the non-linear representation the Lagrangian (1) takes the form

$$\mathcal{L} = \frac{1}{2} \sigma^2 \partial_\mu \vec{U} \partial^\mu \vec{U} + \frac{1}{2} \partial_\mu \sigma \partial^\mu \sigma + \frac{1}{2} m^2 \sigma^2 - \frac{\lambda}{4} \sigma^4. \quad (18)$$

<sup>1</sup> Note that figure 3 shows only the contributions to  $\Phi$  which generate self energies for the  $\phi_i$  modes. In other words, diagrams which consist solely of  $\phi_0$  propagators are not displayed explicitly.

<sup>2</sup> Actually the vertical wiggly line in the tadpole diagrams is still a bare propagator. This subtlety is discussed in the appendix.

Spontaneous symmetry breaking induces a finite vacuum expectation value for the  $\sigma$  mode:

$$\sigma_{\text{vac}} = \sqrt{\frac{m^2}{\lambda}} = v \quad (19)$$

which of course agrees with (4). With the shift

$$\sigma \rightarrow v + \sigma \quad (20)$$

one gets the Lagrangian

$$\mathcal{L}_{\text{non-lin. repr.}} = \frac{1}{2} v^2 \partial_\mu \vec{U} \partial^\mu \vec{U} + v \sigma \partial_\mu \vec{U} \partial^\mu \vec{U} + \frac{1}{2} \sigma^2 \partial_\mu \vec{U} \partial^\mu \vec{U} + \frac{1}{2} \partial_\mu \sigma \partial^\mu \sigma - m^2 \sigma^2 - \lambda v \sigma^3 - \frac{\lambda}{4} \sigma^4. \quad (21)$$

Obviously, the  $\pi$  modes appear only with derivatives. Therefore, all interactions vanish in the limit of soft momenta and no mass terms are induced. This statement is separately true for each conceivable Feynman diagram for the  $\pi$  self energy. Therefore no subtle cancellations are needed to ensure the appearance of Goldstone modes. In any  $\Phi$ -derivable scheme based on (21) the  $\pi$  modes remain massless. Therefore a non-linear representation is better suited for such a resummation scheme. For practical applications the unit vector  $\vec{U}$  must be expanded in powers of the pion field. This is completely analogous to the non-linear sigma model and its extension to chiral perturbation theory [35]. We will not elaborate on this issue here any more. We note, however, that in spite of the chosen non-linear representation in (21) this Lagrangian still describes the linear sigma model since the sigma mode is not frozen, but has a tree level mass as given in (7).

### III. NAMBU–JONA-LASINIO MODEL

As a second example we study the Nambu–Jona-Lasinio (NJL) model [36, 37, 38]. It is widely used as a quark model which possesses the chiral symmetry of QCD. The spontaneous breakdown of this symmetry in vacuum and its restoration at finite temperatures and/or baryon densities has been studied extensively within the NJL model. Also the appearance of Goldstone modes can be studied explicitly within this model. For simplicity we restrict ourselves in the following to two quark flavors. One way to write down the Lagrangian is [37]

$$\mathcal{L} = \bar{q} (i\gamma_\mu \partial^\mu - m - \sigma - i\gamma_5 \pi^a \tau^a) q - \frac{1}{4G} (\sigma^2 + \vec{\pi}^2) \quad (22)$$

with the current quark mass  $m$ .<sup>3</sup> Integrating out the sigma and pion fields (which posses no dynamics at tree level) one obtains the usual NJL Lagrangian with its four-quark couplings.

The NJL model possesses a systematic expansion scheme, namely an expansion in inverse powers of the number of quark colors  $N_c$ . In that context we note that  $G \sim 1/N_c$  (see e.g. [37]). In leading order of the  $1/N_c$  expansion the quarks get a dynamically generated constituent mass (Hartree approximation). The corresponding quark self energy is depicted in figure 4. Note that the solid line in the loop is supposed to be a full quark propagator, i.e. "bubbles within



FIG. 4: Hartree contribution to the quark self energy. The solid lines denote quarks. The double line denotes a bare  $\sigma$  propagator as obtained from the Lagrangian (22), i.e. it is just  $2G$ .

bubbles" are implicitly generated by this diagram. For the mesons, e.g. the pion, the leading order contribution to the self energy is given by the one-loop diagram shown in figure 5(a). Again the solid lines denote full (here Hartree) quark propagators. Note that this quark loop yields also a kinetic term for the pion which is obviously not present at

---

<sup>3</sup> We assume perfect isospin symmetry for simplicity.

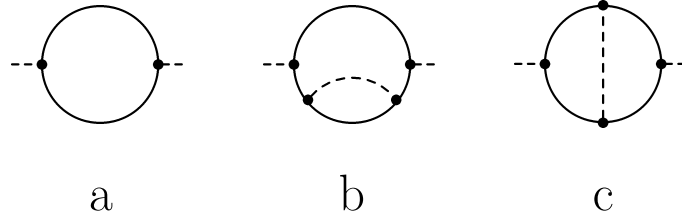


FIG. 5: Perturbative self energy contributions for the pion. Solid lines denote quarks, dashed lines pions.

tree level, i.e. in the Lagrangian (22). This kinetic term is proportional to the square of the pion decay constant (see e.g. [37]).

At leading  $1/N_c$  order the dynamics of the quarks (the generation of a constituent quark mass) influences the meson properties. On the other hand, the dynamics of the mesons are not fed back to influence the quark properties. Actually it is only the expectation value of the sigma, i.e. the one-point function, which causes the Hartree diagram. The connection of tadpoles and one-point functions is discussed from a somewhat more general point of view in the appendix. It is only at next-to-leading order where the meson propagators influence the quark properties. Therefore, processes like quark-quark or quark-meson scattering come into play only at next-to-leading order of the  $1/N_c$  expansion. On the other hand, such processes are of interest e.g. for a dynamical description of the chiral phase transition [39]. From the point of view of a  $\Phi$ -derivable approximation this looks as follows: At leading order in  $1/N_c$  one only has the first (left) diagram shown in figure 6. It is  $O(N_c)$  and generates the Hartree self energy of figure 4. The

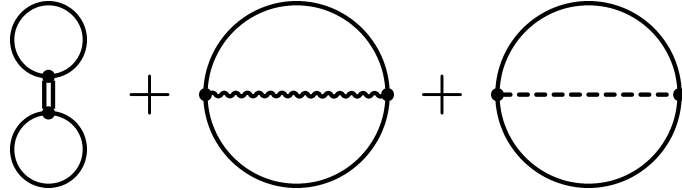


FIG. 6:  $\Phi$ -functional up to  $O(N_c^0)$  for the linear representation (22). All lines denote full propagators except for the double line which is a bare sigma propagator. (This subtlety is explained in the appendix.) Solid lines denote quarks, dashed lines pions and wiggly lines sigmas.

next-to-leading order contributions  $O(N_c^0)$  come from the other two diagrams of figure 6. To generate the mesons and couple the dynamics of quarks and mesons in a selfconsistent way one has to involve (at least) all the diagrams of figure 6. However, as we will discuss next, such a selfconsistent scheme again has problems to ensure that the pions keep their character as Goldstone bosons.

Obviously there is a mass term  $1/(2G)$  for the pion at tree level. In the chiral limit ( $m = 0$ ) this mass term is canceled exactly by the quark loop depicted in figure 5(a), if the quark propagator is determined at the Hartree level depicted in figure 4. For finite quark masses one obtains the Gell-Mann–Oakes–Renner relation [40]. The cancellation between tree level and quark loop does not work any more, if the quark propagator is changed beyond the Hartree level without changing the corresponding vertices. E.g. the  $\Phi$ -derivable approximation depicted in figure 6 generates the perturbative contribution shown in figure 5(b) but *not* the diagram of figure 5(c). Only both diagrams (b) and (c) of figure 5 ensure that the pion remains massless (in the chiral limit). In the following, we will demonstrate how this problem can be circumvented.

Now we turn to a non-linear realization by identifying

$$\sigma + i\tau^a \pi^a = \tilde{\sigma} e^{i\tau^a \pi^a / F} =: \tilde{\sigma} U. \quad (23)$$

We have introduced the pion decay constant  $F$ . To be more specific, at present  $F$  is an arbitrary parameter which drops out of all physical quantities. When a kinetic term for the pion is generated from the loops the free parameter is properly replaced by the pion decay constant  $F_\pi$ . Inserting (23) in (22) we get

$$\begin{aligned} \mathcal{L} &= \bar{q} (i\gamma_\mu \partial^\mu - m - \tilde{\sigma} U P_R - \tilde{\sigma} U^\dagger P_L) q - \frac{1}{4G} \tilde{\sigma}^2 \\ &= \bar{q}_R i\gamma_\mu \partial^\mu q_R + \bar{q}_L i\gamma_\mu \partial^\mu q_L - \bar{q}_L (\tilde{\sigma} U + m) q_R - \bar{q}_R (\tilde{\sigma} U^\dagger + m) q_L - \frac{1}{4G} \tilde{\sigma}^2 \end{aligned} \quad (24)$$

where we have introduced chiral projectors  $P_{R/L} := \frac{1}{2}(1 \pm \gamma_5)$  and right/left handed quarks  $q_{R/L} := P_{R/L} q$ . Obviously, in this non-linear representation of the boson fields there is no pion mass at the tree level. Still it might happen that

a pion mass is generated by loops. In the following, we will demonstrate how to avoid that. To this end, we also change the representation for the quark fields [41, 42]:

$$q'_R = U^{1/2} q_R \quad q'_L = U^{-1/2} q_L. \quad (25)$$

This yields

$$\mathcal{L} = \bar{q}' i\gamma_\mu \partial^\mu q' + \bar{q}'_R iU^{1/2} \gamma_\mu (\partial^\mu U^{-1/2}) q'_R + \bar{q}'_L iU^{-1/2} \gamma_\mu (\partial^\mu U^{1/2}) q'_L - \bar{q}'_L (\tilde{\sigma} + mU^\dagger) q'_R - \bar{q}'_R (\tilde{\sigma} + mU) q'_L - \frac{1}{4G} \tilde{\sigma}^2. \quad (26)$$

In the following, we will only be concerned with the non-linear representation. Therefore we drop from now on the tilde and prime assignment to the fields in (23) and (25). Obviously, in (26) all interactions between the pion fields (encoded in  $U$ ) and the quarks come with derivatives of the pion fields or with the current quark mass. Thus, in the chiral limit soft pions decouple from the quarks. No mass terms for the pion can therefore be generated in any loop order (in the chiral limit). No cancellation of diagrams is needed to achieve that property, since each interaction vertex separately ensures the decoupling of pions.

In powers of  $1/N_c$  the  $\Phi$ -derivable approximation shown in figure 6 (using the linear representation (22)) yields the generating functional up to  $O(N_c^0)$ . The same accuracy can be obtained in the non-linear representation, if all  $U$ 's appearing in (26) are expanded up to  $O(1/F^2)$ . Note that  $F^2 \sim N_c$  which can be easily obtained from the Gell-Mann–Oakes–Renner relation. We obtain

$$\mathcal{L} \approx \bar{q} \left( i\gamma_\mu \partial^\mu - m - \sigma + \frac{1}{2F} \gamma_\mu \partial^\mu \pi^a \tau^a \gamma_5 + \frac{m}{2F^2} \tilde{\sigma}^2 + \frac{im}{F} \gamma_5 \pi^a \tau^a \right) q - \frac{1}{4G} \sigma^2. \quad (27)$$

Actually there emerges one more term with two pion fields, the Weinberg–Tomozawa term  $\sim \bar{q} \gamma^\mu \epsilon^{abc} \pi^a \partial_\mu \pi^b \tau^c q$ . On the level of approximation which we treat in figure 7, this term enters the calculation of  $\Phi$  only as a tadpole type contribution. Since the Weinberg–Tomozawa term is flavor changing, this tadpole vanishes (as long as there is no isospin chemical potential). Of course, this would change, if we were interested in a calculation of  $\Phi$  beyond  $O(N_c^0)$ .

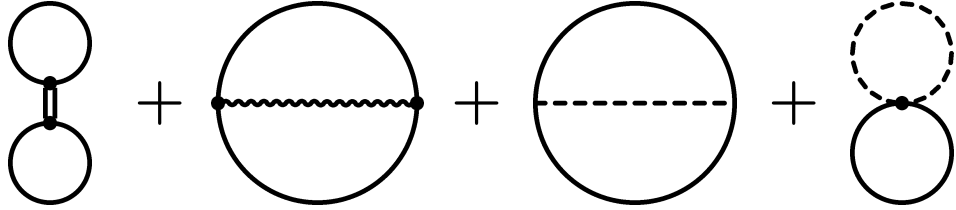


FIG. 7:  $\Phi$ -functional up to  $O(N_c^0)$  for the non-linear representation (27). All lines denote full propagators except for the double line which is a bare sigma propagator (cf. figure 6 and the appendix). Solid lines denote quarks, dashed lines pions and wiggly lines sigmas. The three-point pion-quark vertex consists of two parts depicted in figure 8.

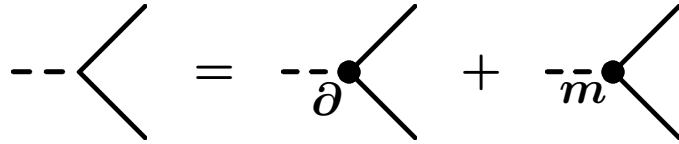


FIG. 8: Pion-quark vertices of the non-linear representation (27). Solid lines denote quarks, dashed lines pions.

The pion mass  $M_\pi$  is obtained from the self energy diagrams depicted in figure 9. Obviously, diagrams (a), (b), (c) and (d) are proportional to  $M_\pi^2$ ,  $mM_\pi$ ,  $m^2$  and  $m$ , respectively. Thus, comparing diagrams (a) and (d) yields  $M_\pi^2 \sim m$  and diagrams (b) and (c) are only subleading corrections. Indeed, it is easy to see that the correct Gell-Mann–Oakes–Renner relation emerges from diagrams (a) and (d): The quark condensate appears in diagram (d), together with the vertex  $\sim m$ . On the other hand, diagram (a) is caused by the pseudovector interaction in (27) which couples the derivative of the pion field to the axial-vector current. The latter defines the pion decay constant. Thus,  $M_\pi^2 F_\pi^2$  emerges from diagram (a). We conclude that the Goldstone boson character of the pion is respected in a  $\Phi$ -derivable approach to the NJL model, if the starting point is the Lagrangian (26) instead of (22). Therefore, the non-linear representation is clearly better suited for studies of the low-temperature phase where chiral symmetry is spontaneously broken. However, it is important to note that there is one aspect where the linear representation has its merits: In

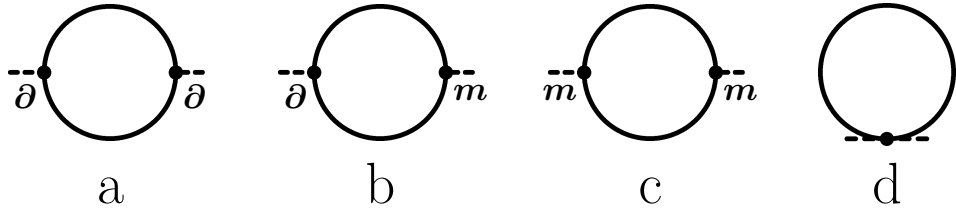


FIG. 9: Pion self energy obtained in the non-linear representation from the  $\Phi$ -functional shown in figure 7. Note that all internal lines denote full propagators.

(22) one can clearly see the chiral partners of the model,  $\sigma$  and  $\vec{\pi}$ , which become degenerate for temperatures above the phase transition [37]. Naturally, a non-linear representation does not display the chiral partners so explicitly. What makes the use of the non-linear representation at the technical level rather involved close to or even above the phase transition can be understood as follows: We have argued that a proper expansion parameter is  $1/F$  to come from (26) to the practically useful Lagrangian (27). Close to the chiral transition the relevant  $F$  becomes small, however. Therefore, an expansion in  $1/F$  ceases to be useful. A numerical study of the  $\Phi$ -functional shown in figure 7 as a function of the temperature is beyond the scope of the present work. At least for temperatures below the chiral transition the non-linear representation is an appropriate tool as it respects the Goldstone boson character of the pions also within resummation schemes.

#### IV. VECTOR MESONS AND CURRENT CONSERVATION

We now turn to a different problem encountered in resummation schemes, namely the violation of current conservation for systems with massive vector mesons. Typically vector mesons are described by a Lorentz vector field  $V_\mu$  which has four indices. On the other hand, a massive vector meson has only three polarizations. The (free) equation of motion (Proca equation [43]) is then constructed such that one component of the vector field is frozen by the condition

$$\partial^\mu V_\mu = 0. \quad (28)$$

If interactions are switched on and the vector mesons are only coupled to currents  $j_\mu$  which are conserved, then (28) remains valid in the presence of these interactions — at least for a full solution of the quantum field theoretical problem. However, the conservation of  $j_\mu$  is typically a consequence of an internal symmetry which on the level of  $n$ -point functions connects propagators and vertices (an example is discussed in [6]). For approximate solutions and especially using resummation schemes it might therefore appear that current conservation is spoiled. As a consequence also (28) is violated and the current non-conservation is proliferated by the now non-vanishing longitudinal mode of the vector meson. Recipes how to tame such problems and the appearance of possible new problems caused by the use of such recipes are discussed in [6, 44, 45, 46, 47]. In the following we will demonstrate how the problem of current non-conservation can be circumvented by a different choice of representation for the vector meson field.

We start with the vector meson Lagrangian

$$\mathcal{L} = -\frac{1}{4} F_{\mu\nu} F^{\mu\nu} + \frac{1}{2} m^2 V_\mu V^\mu + V_\mu j^\mu \quad (29)$$

with a source term  $j^\mu$  and the field strength  $F_{\mu\nu} = \partial_\mu V_\nu - \partial_\nu V_\mu$ . Interactions of the vector mesons with other fields can be encoded in  $j^\mu$ . Note that typical interactions of vector mesons with other fields can be written in the way (29). However, it is not the most general case: Also terms like  $V_\mu V_\nu j^{\mu\nu}$  are conceivable. Indeed, if vector meson masses are generated via a Higgs field  $\phi$  [48], terms with  $j^{\mu\nu} \sim g^{\mu\nu} \phi^2$  appear. Terms with two vector fields in the interaction part are unfortunately not suitable for the field redefinitions which we discuss below. Therefore, our framework does not cover the case of dynamical vector meson mass generation and, as we will see below, also not the case of massless vector mesons. Nonetheless, the Lagrangian (29) covers a large body of frequently used hadronic Lagrangians with vector mesons. Concerning field redefinitions for vector states we also refer to appendix B in [49].

We introduce a new antisymmetric tensor field  $\bar{F}_{\mu\nu}$  and study the new Lagrangians

$$\mathcal{L}' = \frac{1}{4} \bar{F}_{\mu\nu} \bar{F}^{\mu\nu} + \frac{1}{2} m^2 V_\mu V^\mu - \bar{F}_{\mu\nu} \partial^\mu V^\nu + V_\mu j^\mu \quad (30)$$

and

$$\mathcal{L}'' = \frac{1}{4} \bar{F}_{\mu\nu} \bar{F}^{\mu\nu} + \frac{1}{2} m^2 V_\mu V^\mu + V^\mu (j_\mu + \partial^\nu \bar{F}_{\nu\mu}) . \quad (31)$$

Since  $\bar{F}_{\mu\nu}$  appears at most in quadratic order in (30) this field can be integrated out. Since there are no derivatives acting on this field one obtains again a local action. Actually, one ends up with the original Lagrangian (29). On the other hand, the Lagrangians (30) and (31) differ only by an irrelevant total derivative. Thus all three Lagrangians are equivalent. In (31) the field  $V_\mu$  appears only up to quadratic order and without derivatives acting on it. Hence,  $V_\mu$  can be easily integrated out. One gets

$$\mathcal{L}'' \rightarrow \frac{1}{4} \bar{F}_{\mu\nu} \bar{F}^{\mu\nu} - \frac{1}{2m^2} \partial^\nu \bar{F}_{\nu\mu} \partial_\alpha \bar{F}^{\alpha\mu} - \frac{1}{m^2} j^\mu \partial^\nu \bar{F}_{\nu\mu} - \frac{1}{2m^2} j_\mu j^\mu . \quad (32)$$

To achieve a proper normalization of the kinetic terms we introduce  $\bar{F}_{\mu\nu} =: m V_{\mu\nu}$  and obtain

$$\mathcal{L}_{\text{tensor repr.}} = \frac{1}{4} m^2 V_{\mu\nu} V^{\mu\nu} - \frac{1}{2} \partial^\nu V_{\nu\mu} \partial_\alpha V^{\alpha\mu} - \frac{1}{m} j^\mu \partial^\nu V_{\nu\mu} - \frac{1}{2m^2} j_\mu j^\mu . \quad (33)$$

The first two terms on the right hand side are just the mass and kinetic term of the free Lagrangian for vector fields in the tensor representation [35, 50, 51]. The other two terms represent the interaction of the vector field with the source and a quadratic source term. The latter induces a point interaction, if the source is expressed in terms of the fields the vectors are supposed to interact with.

In contrast to the original interaction term  $V_\mu j^\mu$  the new interaction term  $j^\mu \partial^\nu V_{\nu\mu}$  automatically projects on transverse states:

$$j^\mu \partial^\nu V_{\nu\mu} = j^\mu \left( \underbrace{g_{\mu\alpha} - \frac{\partial_\mu \partial_\alpha}{\partial^2}}_{P_{\mu\alpha}^T} + \underbrace{\frac{\partial_\mu \partial_\alpha}{\partial^2}}_{P_{\mu\alpha}^L} \right) \partial_\nu V^{\nu\alpha} = j^\mu P_{\mu\alpha}^T \partial_\nu V^{\nu\alpha} \quad (34)$$

where we have used

$$\partial_\alpha \partial_\nu V^{\nu\alpha} = 0 \quad (35)$$

which holds since  $V^{\nu\alpha}$  has been introduced as an antisymmetric tensor. Obviously problems with current conservation are now no longer proliferated by the vector mesons. Therefore a tensor representation for the vector mesons provides a better starting point for selfconsistent approximations than the frequently used vector representation.

Trading a vector field with one Lorentz index with a tensor field with two indices, one might get the feeling that in practice this becomes technically rather difficult. However, such kind of difficulties always have a simple solution: One just needs the proper projectors to decompose everything in scalar quantities (times projectors). Without much details we present in the following the projectors for the tensor representation which are required for (equilibrium) in-medium calculations, i.e. for a situation where one has a Lorentz vector  $p$  which specifies the medium. In such a case one can distinguish vector mesons which move with respect to the medium from those which do not. (In vacuum one can always boost to the frame where the vector meson is at rest.) For moving (massive) vector mesons one can distinguish their respective polarization [52]: Either it is longitudinal (l) or transverse (t) with respect to the three-momentum of the vector meson. (We recall that the polarization is always transverse (T) with respect to the four-momentum.)

The pertinent tensor structures are: the unity tensor

$$P_1^{\mu\nu\alpha\beta} = \frac{1}{2} (g^{\mu\alpha} g^{\nu\beta} - g^{\mu\beta} g^{\nu\alpha}) , \quad (36)$$

the tensor transverse with respect to the four-momentum  $k$

$$P_T^{\mu\nu\alpha\beta} = \frac{1}{2k^2} (g^{\mu\alpha} k^\nu k^\beta - g^{\mu\beta} k^\nu k^\alpha - g^{\nu\alpha} k^\mu k^\beta + g^{\nu\beta} k^\mu k^\alpha) , \quad (37)$$

the tensor longitudinal with respect to the four-momentum  $k$

$$P_L = P_1 - P_T , \quad (38)$$

the tensor transverse with respect to the four-momentum  $k$  and longitudinal with respect to the three-momentum<sup>4</sup>  $\vec{k}$

$$P_l^{\mu\nu\alpha\beta} = \frac{1}{2(k^2 p^2 - (k \cdot p)^2)} (k^\mu k^\alpha p^\nu p^\beta - k^\mu k^\beta p^\nu p^\alpha - k^\nu k^\alpha p^\mu p^\beta + k^\nu k^\beta p^\mu p^\alpha) \quad (39)$$

and the tensor transverse with respect to four- and three-momentum

$$P_t = P_T - P_l. \quad (40)$$

Obviously all tensors are constructed such that they are antisymmetric with respect to an exchange of the first (third) and the second (fourth) index. This just reflects the property of the basic object, the *antisymmetric* tensor field  $V_{\mu\nu}$ .

It is easy to check that the following relations hold:

$$P_i \otimes P_i = P_i \quad \text{for } i = 1, T, L, t, l; \quad (41a)$$

$$P_1 \otimes P_i = P_i \otimes P_1 = P_i \quad \text{for } i = L, T, t, l; \quad (41b)$$

$$P_L \otimes P_i = P_i \otimes P_L = 0 \quad \text{for } i = T, t, l; \quad (41c)$$

$$P_T \otimes P_i = P_i \otimes P_T = P_i \quad \text{for } i = t, l; \quad (41d)$$

$$P_l \otimes P_t = P_t \otimes P_l = 0 \quad (41e)$$

where the product “ $\otimes$ ” is of course defined by contracting the last two indices of the first tensor with the first two indices of the second tensor.

The free propagator is given by [50]

$$\langle 0 | T V^{\mu\nu}(x) V^{\alpha\beta}(y) | 0 \rangle = i \int \frac{d^4 k}{(2\pi)^4} e^{-ik(x-y)} \left( -\frac{2}{k^2 - m^2} P_T^{\mu\nu\alpha\beta} + \frac{2}{m^2} P_L^{\mu\nu\alpha\beta} \right) \quad (42)$$

which shows that only transverse (T) modes are propagated while the longitudinal (L) mode is frozen. Of course, for a free propagator there is no distinction between transverse (t) and longitudinal (l) polarizations.

Finally we note that we have nothing clever to say about *massless* vector mesons: From (33) it is obvious that the transformations which lead from the original Lagrangian (29) to (33) only work for  $m \neq 0$ . Therefore, the formalism developed in the present section does not work for massless vector states (and, as already discussed at the beginning of this section, also not for the case where the mass is dynamically generated). The formalism does work, however, for typical hadronic Lagrangians involving massive vector mesons.

### Acknowledgments

The author acknowledges stimulating discussions with F. Frömel, J. Knoll, A. Peshier, D. Rischke and J. Schaffner-Bielich. He also thanks U. Mosel for continuous support.

### APPENDIX A: TADPOLES IN $\Phi$ -DERIVABLE APPROACHES

The  $\Phi$ -derivable scheme deals with full two-point functions. Here tadpoles are somewhat special since they are connected to one-point functions. To illustrate the point we consider a simple model with two distinct scalar fields:

$$\mathcal{L} = \frac{1}{2} \partial_\mu \phi \partial^\mu \phi + \frac{1}{2} \partial_\mu \varphi \partial^\mu \varphi - \frac{1}{2} M^2 \phi^2 - \frac{1}{2} m^2 \varphi^2 - \frac{1}{2} g \phi \varphi^2. \quad (A1)$$

In general, the generating functional to which  $\Phi$  contributes must be considered as a functional of one- and two-point functions and not only of two-point functions. It is given by [5]

$$\Gamma[\phi_c, \varphi_c, D_\phi, D_\varphi] = \underbrace{\int d^4 x \mathcal{L}[\phi_c, \varphi_c]}_{=S_c[\phi_c, \varphi_c]} + \Phi[\phi_c, \varphi_c, D_\phi, D_\varphi] + \text{terms independent of } \phi_c, \varphi_c. \quad (A2)$$

---

<sup>4</sup> The three-momentum is measured relative to the medium characterized by  $p$ . A Lorentz covariant expression for the three-momentum is given by  $k - \frac{k \cdot p}{p^2} p$ .

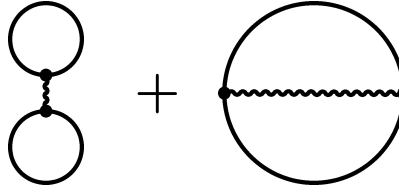


FIG. 10:  $\Phi$ -functional in two-loop order for the  $\phi\varphi^2$  model. Solid lines denote  $\varphi$  modes, wiggly lines  $\phi$  modes. It will turn out that the wiggly line in the left diagram must be a bare (non-dynamical) propagator, whereas the wiggly line in the right diagram is a full propagator. See main text for details.

Here,  $\mathcal{O}_c$  denote one-point functions (classical fields) and  $D_{\mathcal{O}}$  propagators.  $\Phi$  is now given by all two-particle irreducible diagrams. These are all diagrams which do not fall apart, if two lines are cut. In particular, the left diagram of figure 10 — the tadpole diagram — does *not* enter here, since it already falls apart after cutting one line. On the other hand, tadpole diagrams do show up in perturbative evaluations of the self energy. So the question emerges: Where are the tadpole diagrams in the  $\Phi$ -approach? Indeed, a tadpole type diagram does emerge, but it is not the left diagram of figure 10. Instead, the diagram depicted in figure 11 must be considered (cf. also [5]). Note that here the wiggly line



FIG. 11: Contribution to the  $\Phi$ -functional taking into account one-point functions in the  $\phi\varphi^2$  model. The solid line denotes a propagator of the  $\varphi$  mode, the wiggly line plus cross a one-point function of the  $\phi$  mode. See main text for details.

cannot be cut, since the cross together with the line denotes one object, namely  $\phi_c$ . Of course, the right diagram of figure 10 and higher loop orders contribute to  $\Phi$ . All these diagrams, however, do not contain  $\phi_c$  (in our simple toy model (A1)). The contribution of figure 11 to the  $\Phi$ -functional is given by

$$\Phi_{\text{figure 11}} = -\frac{1}{2} \int d^4x g \phi_c(x) D_{\varphi}(x, x). \quad (\text{A3})$$

In the following we are aiming at a generating functional for the two-point functions only. In other words, we want to write down a  $\Phi$ -functional which only depends on the propagators and not any more on the classical fields. Of course, this new  $\Phi$ -functional still should yield the correct self energy for the Dyson-Schwinger equation. To derive this new  $\Phi$ -functional all we have to do is to solve the equations of motion for the classical fields and plug the solutions in  $S_c[\phi_c, \varphi_c] + \Phi[\phi_c, \varphi_c, D_{\phi}, D_{\varphi}]$  which appears in (A2).

The equation of motion for  $\varphi_c$  is given by

$$0 = \frac{\delta \Gamma}{\delta \varphi_c} = -\partial_x^2 \varphi_c(x) - m^2 \varphi_c(x) - g \phi_c(x) \varphi_c(x). \quad (\text{A4})$$

In a thermal system expectation values are independent of the coordinate. We do not consider spontaneous symmetry breaking for the  $\varphi$  mode and conclude:  $\varphi_c = 0$ . The equation of motion for  $\phi_c$  is more involved:

$$0 = \frac{\delta \Gamma}{\delta \phi_c} = -\partial_x^2 \phi_c(x) - M^2 \phi_c(x) - \frac{1}{2} g \varphi_c^2(x) - \frac{1}{2} g D_{\varphi}(x, x). \quad (\text{A5})$$

The last term on the right hand side of (A5) is exactly the contribution generated from the diagram in figure 11. Again, in a thermal system also  $\phi_c$  is independent of the coordinate. Using  $\varphi_c = 0$  one gets

$$\phi_c = -\frac{g}{2M^2} D_{\varphi}(x, x). \quad (\text{A6})$$

The factor  $1/M^2$  should be interpreted as a *bare* (or non-dynamical)  $\phi$  propagator which couples to the closed loop  $D_{\varphi}(x, x)$ . Since  $\phi_c$  can be determined exactly, one can insert the solution in (A2) and obtain a generating functional for the two-point functions only. The terms caused by  $\phi_c$  are

$$S_c[\phi_c, \varphi_c] + \Phi_{\text{figure 11}}[\phi_c, D_{\varphi}] = \int d^4x \left[ -\frac{1}{8} \frac{g^2}{M^2} [D_{\varphi}(x, x)]^2 + \frac{1}{4} \frac{g^2}{M^2} [D_{\varphi}(x, x)]^2 \right] = \frac{1}{8} \int d^4x \frac{g^2}{M^2} [D_{\varphi}(x, x)]^2. \quad (\text{A7})$$

By inspection of this last formula we see that in this way the left diagram of figure 10 emerges with a subtle, but important aspect: The wiggly line is a *bare* propagator and not a full one.<sup>5</sup> In this way, taking the derivative of this diagram with respect to  $D_\phi$  yields zero, since there is no full  $\phi$  propagator. On the other hand, taking a derivative with respect to  $D_\varphi$  yields the tadpole diagram.

We have chosen the simple model (A1) to illustrate in which way tadpole diagrams enter the  $\Phi$ -formalism. In our simple case the equations of motion for the classical fields could be solved exactly. This can be different for more complicated theories. What is generic, however, is the fact that in a  $\Phi$ -functional of propagators only, tadpole diagrams must be included, but with “tadpole tails” which are bare and not full propagators.

The same line of reasoning applies to the models discussed in sections II and III.

---

[1] G. Baym, Phys. Rev. **127**, 1391 (1962).  
 [2] J. M. Luttinger and J. C. Ward, Phys. Rev. **118**, 1417 (1960).  
 [3] J. M. Cornwall, R. Jackiw, and E. Tomboulis, Phys. Rev. **D10**, 2428 (1974).  
 [4] W. Weinhold, B. Friman, and W. Nörenberg, Phys. Lett. **B433**, 236 (1998), nucl-th/9710014.  
 [5] Y. B. Ivanov, J. Knoll, and D. N. Voskresensky, Nucl. Phys. **A657**, 413 (1999), hep-ph/9807351.  
 [6] H. van Hees and J. Knoll, Nucl. Phys. **A683**, 369 (2000), hep-ph/0007070.  
 [7] H. van Hees and J. Knoll, Phys. Rev. **D65**, 025010 (2002), hep-ph/0107200.  
 [8] H. Van Hees and J. Knoll, Phys. Rev. **D65**, 105005 (2002), hep-ph/0111193.  
 [9] H. van Hees and J. Knoll, Phys. Rev. **D66**, 025028 (2002), hep-ph/0203008.  
 [10] Y. B. Ivanov, F. Riek, H. van Hees, and J. Knoll, Phys. Rev. **D72**, 036008 (2005), hep-ph/0506157.  
 [11] J. P. Blaizot, E. Iancu, and A. Rebhan, Phys. Lett. **B470**, 181 (1999), hep-ph/9910309.  
 [12] J. P. Blaizot, E. Iancu, and A. Rebhan, Phys. Rev. **D63**, 065003 (2001), hep-ph/0005003.  
 [13] J. P. Blaizot, E. Iancu, and A. Rebhan, Nucl. Phys. **A698**, 404 (2002), hep-ph/0104033.  
 [14] J.-P. Blaizot, E. Iancu, and U. Reinosa, Phys. Lett. **B568**, 160 (2003), hep-ph/0301201.  
 [15] J.-P. Blaizot, E. Iancu, and U. Reinosa, Nucl. Phys. **A736**, 149 (2004), hep-ph/0312085.  
 [16] A. Peshier, B. Kampfer, O. P. Pavlenko, and G. Soff, Europhys. Lett. **43**, 381 (1998), hep-ph/9801344.  
 [17] A. Peshier, Phys. Rev. **D63**, 105004 (2001), hep-ph/0011250.  
 [18] A. Peshier, Nucl. Phys. **A702**, 128 (2002), hep-ph/0110342.  
 [19] G. Aarts, D. Ahrensmeier, R. Baier, J. Berges, and J. Serreau, Phys. Rev. **D66**, 045008 (2002), hep-ph/0201308.  
 [20] J. Berges, Phys. Rev. **D70**, 105010 (2004), hep-ph/0401172.  
 [21] M. Alford, J. Berges, and J. M. Cheyne, Phys. Rev. **D70**, 125002 (2004), hep-ph/0404059.  
 [22] J. Berges, S. Borsanyi, U. Reinosa, and J. Serreau, Annals Phys. **320**, 344 (2005), hep-ph/0503240.  
 [23] J. Berges, S. Borsanyi, U. Reinosa, and J. Serreau, Phys. Rev. **D71**, 105004 (2005), hep-ph/0409123.  
 [24] D. Roder, J. Ruppert, and D. H. Rischke, Phys. Rev. **D68**, 016003 (2003), nucl-th/0301085.  
 [25] D. Roder, J. Ruppert, and D. H. Rischke (2005), hep-ph/0503042.  
 [26] J. T. Lenaghan, D. H. Rischke, and J. Schaffner-Bielich, Phys. Rev. **D62**, 085008 (2000), nucl-th/0004006.  
 [27] J. T. Lenaghan and D. H. Rischke, J. Phys. **G26**, 431 (2000), nucl-th/9901049.  
 [28] S. Kamefuchi, L. O’Raifeartaigh, and A. Salam, Nucl. Phys. **28**, 529 (1961).  
 [29] H. W. Fearing and S. Scherer, Phys. Rev. **C62**, 034003 (2000), nucl-th/9909076.  
 [30] S. Scherer and H. W. Fearing, Phys. Rev. **D52**, 6445 (1995), hep-ph/9408298.  
 [31] G. Chanfray, M. Ericson, and P. A. M. Guichon, Phys. Rev. **C63**, 055202 (2001), nucl-th/0012013.  
 [32] J. Goldstone, A. Salam, and S. Weinberg, Phys. Rev. **127**, 965 (1962).  
 [33] J. Goldstone, Nuovo Cim. **19**, 154 (1961).  
 [34] T. Matsubara, Prog. Theor. Phys. **14**, 351 (1955).  
 [35] J. Gasser and H. Leutwyler, Ann. Phys. **158**, 142 (1984).  
 [36] U. Vogl and W. Weise, Prog. Part. Nucl. Phys. **27**, 195 (1991).  
 [37] S. P. Klevansky, Rev. Mod. Phys. **64**, 649 (1992).  
 [38] T. Hatsuda and T. Kunihiro, Phys. Rept. **247**, 221 (1994), hep-ph/9401310.  
 [39] P. Rehberg, L. Bot, and J. Aichelin, Nucl. Phys. **A653**, 415 (1999), hep-ph/9809565.  
 [40] M. Gell-Mann, R. J. Oakes, and B. Renner, Phys. Rev. **175**, 2195 (1968).  
 [41] D. Espriu, E. de Rafael, and J. Taron, Nucl. Phys. **B345**, 22 (1990), erratum-ibid. **B355**, 278 (1991).  
 [42] A. Manohar and H. Georgi, Nucl. Phys. **B234**, 189 (1984).  
 [43] U. Mosel, *Fields, symmetries, and quarks* (Springer, 1999).

---

<sup>5</sup> This is similar to the non-relativistic case discussed in [53]. There, in appendix C it is pointed out that also the classical potential must not be regarded as a dynamical quantity, i.e. it should not be considered/cut when calculating derivatives with respect to the full propagator.

- [44] F. Riek and J. Knoll, Nucl. Phys. **A740**, 287 (2004), nucl-th/0402090.
- [45] J. Ruppert and T. Renk, Phys. Rev. **C71**, 064903 (2005), nucl-th/0412047.
- [46] F. Riek, H. van Hees, and J. Knoll (2006), nucl-th/0607023.
- [47] J. Ruppert and T. Renk (2006), nucl-th/0609082.
- [48] M. E. Peskin and D. V. Schroeder, *An Introduction to Quantum Field Theory* (Perseus, Cambridge, Massachusetts, 1995).
- [49] B. Borasoy and U.-G. Meissner, Int. J. Mod. Phys. **A11**, 5183 (1996), hep-ph/9511320.
- [50] G. Ecker, J. Gasser, A. Pich, and E. de Rafael, Nucl. Phys. **B321**, 311 (1989).
- [51] G. Ecker, J. Gasser, H. Leutwyler, A. Pich, and E. de Rafael, Phys. Lett. **B223**, 425 (1989).
- [52] C. Gale and J. I. Kapusta, Nucl. Phys. **B357**, 65 (1991).
- [53] Y. B. Ivanov, J. Knoll, and D. N. Voskresensky, Nucl. Phys. **A672**, 313 (2000), nucl-th/9905028.